Electronic structure of ideal $TiO_2(110)$, $TiO_2(001)$, and $TiO_2(100)$ surfaces

S. Munnix and M. Schmeits
Institut de Physique, Université de Liège, B-4000 Sart Tilman (Liège) 1, Belgium
(Received 23 December 1983)

We report theoretical investigations on the electronic structure of ideal, defect-free surfaces of rutile (TiO_2). The (110), (001), and (100) faces are studied, and for each face, several models are examined, which correspond to different surface atomic compositions. The bulk electronic structure is described by a tight-binding Hamiltonian including interactions up to second-nearest neighbors. From this, the surface electronic structure is determined by making use of the scattering-theoretic method. The results are obtained in terms of surface bound states, surface resonances, and surface densities of states, which are wave-vector, layer, atom, and orbital resolved. This allows a detailed discussion of the origin, the nature, and the localization of the various surface features obtained. For all surface models examined, no occupied states are found in the gap, in accordance with experimental results. The main effect of the surface is to induce O p—derived resonances in the valence-band region and Ti d—derived resonances in the conduction-band region. These trends are correlated with the relatively strong ionicity of TiO_2. The nature and the strength of the surface states and resonances, as well as their variation from one face to the other are interpreted in terms of the coordination of the surface cations, the removal of anion second-nearest neighbors, and the reduced screening of cation-cation interactions due to the removal of surface anions.

I. INTRODUCTION

During the past decade, theoretical studies on the electronic structure of semiconductor surfaces were mainly concerned with tetrahedrally bonded semiconductors, such as Si, Ge, GaAs, and ZnO, whose valence and conduction bands essentially originate from the sp^3 hybrid orbitals of their constituting atoms. Titanium dioxide differs in two aspects from these materials. First, it crystallizes with the bulk rutile structure, which contains two titanium and four oxygen atoms per unit cell (see Fig. 1); henceforth, its coordination is 6:3. Secondly, the chemical bonding is governed by the interaction between the oxygen $2p$ and titanium $3d$ states, which leads to a wide-gap semiconductor ($E_g = 3$ eV) of relatively strong ionicity. A theoretical study of TiO_2-surface electronic properties is thus of fundamental interest. In addition, TiO_2 surfaces play an important role in numerous technological applications, like photovoltaic cells,[1] as well as in a number of catalytic and electrochemical processes, such as the photolysis of water and the oxidation and reduction of organic and inorganic molecules.[2,3]

A. Experimental background

Since 1916, rutile is known to be one of the three polymorphic structures of TiO_2, the two other ones being anatase and brookite.[4] Its general physical properties have been widely investigated since then. Surface properties have been the subject of extensive experimental work, the main results of which have been reviewed by Henrich.[5] Measurements have been done on the (110) and (100) faces under various experimental conditions: by preparing the surfaces by different methods (cleaving or fracturing, with or without annealing at different temperatures), and by measuring surface properties before and after Ar-ion bombardment, before and after adsorption of atomic or molecular species.[5]

We will now briefly recall those results which are of direct concern for our work. Tait and Kasowski,[6] Chung *et al.*,[7] van Steertegem *et al.*,[8] and Henrich *et al.*[9,10] performed low-energy electron diffraction (LEED), electron-energy-loss spectroscopy (EELS), and ultraviolet photoelectron spectroscopy (UPS) on the various faces under consideration. LEED patterns reveal the (110) face to have a stable (1×1) unreconstructed structure after annealing at 600—800 °C. The (001) face is unstable upon annealing and gives rise to reconstruction of faceting.[11] The (100) face leads to (1×1) (Ref. 8), (1×3), (1×5), or (1×7) (Refs. 7 and 8) reconstruction patterns after annealing. For fractured, unannealed surfaces of various orientations, Henrich and Kurtz[10] obtained LEED patterns characteristic of an unreconstructed surface, but these LEED patterns were very poor, revealing a high density of surface defects. In conclusion, unreconstructed phases exist for all three faces, but in some cases, an appreciable amount of surface defects may be present.

EELS measurements on unreconstructed, defect-free surfaces yield no peaks at energies below the gap value ($E_g = 3.0$ eV), indicating that all transitions occur from the valence-band to the conduction-band region. Transitions at lower energies, related to states inside the gap, are detected only for surfaces containing defects, as is the case after Ar-ion bombardment, unannealed fracturing, or Ti deposition.

UPS spectra from vacuum-fractured (110), (001), and (100) surfaces show a weak emission from gap states, located from 1.0 to 0.6 eV below the conduction-band edge. After annealing, this emission almost completely disappears. It is, however, strongly enhanced when the surface

has been bombarded with Ar ions or with energetic electrons. This emission is associated with an oxygen deficiency at the surface. Actually, Auger analysis[6] shows that the Ti/O ratio increases with Ar-ion bombardment and decreases with increasing annealing temperature, as O diffusion from inside the crystal restores the original bulk stoichiometry at the surface.

In summary, we can say that on unreconstructed, clean TiO_2 surfaces, no surface state is experimentally detected in the gap. The emission from surfaces presenting defects is generally assigned to (Ti^{3+})—(O vacancy) complexes,[10] although the exact nature of these defects is not precisely known.

B. Theoretical framework

Recently, we have published preliminary results of theoretical investigations on the TiO_2-surface electronic structure.[12] This work is devoted to a detailed systematic study of the ideal, defect-free (110), (001), and (100) surfaces. We consider "flat" surfaces (i.e., cut exactly along a crystallographic plane), with atoms held at their bulk position. For each surface orientation, several atomic planes may terminate the surface, due to the structure of the bulk lattice. For the (110) face, we present two different surface models. In the first one, the surface layer is the most compact atomic plane, which contains two Ti and two O atoms per surface unit cell. This model was chosen by analogy with the surface composition suggested by de Frésart *et al.*[13] for the (110) surface of SnO_2, a material which also crystallizes with the rutile structure. In the second model, an additional oxygen layer terminates the semi-infinite solid, as would result from a symmetrical cut of the crystal. This model has been widely used in the literature, as in this way, the smallest number of anion-cation bonds are broken (see Ref. 10). For the (001) surface, only one model has to be considered, as the topmost layer always contains one Ti and two O atoms per unit cell. In the case of the (100) surface, each layer contains only one atom per surface unit cell, each titanium layer being followed by two oxygen layers as one moves in towards the crystal. Thus, depending on which plane terminates the solid, three models are possible: (Ti—O—O— $\cdots$), (O—Ti—O— $\cdots$), or (O—O—Ti— $\cdots$). The electronic structures of these three models will be compared, allowing the simulation of different experimental conditions, where more or less oxygen is adsorbed or desorbed.

It is impossible to determine which of the models considered here describes the true surface composition with the present state of knowledge. The actual surface atomic structure could be obtained from certain experimental results, like dynamical LEED analysis, as has been done for several III-V semiconductors,[14] but to our knowledge, there are no such results currently available for TiO_2. Furthermore, surface relaxation is expected to occur, and this effect should be taken into account in order to study realistic surfaces. Unfortunately, we again lack experimental information on the exact positions of the relaxed atoms, needed as input data for our investigations. But from surface-electronic-structure studies on other polar materials, such as ZnO,[15] it is known that no large atomic displacements occur at the surfaces of ionic material, and that the quantitative changes in the surface electronic structure upon relaxation are less important for these materials than for more covalent semiconductors.

For each surface model under consideration, the surface electronic structure is obtained by application of the scattering theoretic method (STM).[16] In this method, the bulk crystal is described by a tight-binding linear combination of atomic orbitals Hamiltonian, including interactions up to second-nearest neighbors. The surface is then created by removing as many atomic layers as necessary in order to decouple the remaining two semi-infinite crystals. As the amount of computational effort needed depends essentially on the spatial extent of the perturbation, the problem remains numerically tractable,[17] even for crystals such as TiO_2 with a large unit cell. This is an essential advantage as compared to cluster or slab methods, where large numbers of atoms or layers have to be considered in order to realistically simulate an infinite half crystal, and where the numerical effort increases with cluster or slab thickness. In addition, in such methods, redundant surface states or interference effects may arise, due to the finite cluster or slab size, whereas the STM exactly describes the effect of a surface limiting a semi-infinite solid. The application of the STM requires the computation of the bulk Green's function in an appropriate basis depending on the surface orientation considered. Once this computation has been performed for a given orientation, several surface models may be studied without appreciable further work, as will be seen in the sections below. The results are obtained in terms of bound surface states, surface resonances and antiresonances, and surface densities of states which are resolved with respect to the two-dimensional wave vector $\vec{q}$ as well as with respect to the atomic layer, atomic position, and orbital composition.

The method has been applied with success to Si, Ge, GaAs,[16] and ZnO,[15] where it has proved to yield not only a detailed and sound qualitative description of surface effects, but also results which are in quantitative agreement with angle-resolved UPS measurements. It may be extended to the case of relaxed and reconstructed surfaces, as has been done e.g., for GaAs(110) and Si(100)-(2×1).[18]

The paper is organized as follows: In Sec. II, we will give a description of the bulk electronic structure, which will serve as a starting point to investigate surface properties. Section III briefly recalls the formal developments of the STM. In Secs. IV, V, and VI we report in detail the results of our surface-electronic-structure calculations for the three faces under consideration. In Sec. VII, we discuss extensively the results obtained, interpreting them in terms of the underlying bulk electronic structure and of the chemical bonding of the surface atoms. The influence of the material's ionicity and of the coordination of the surface cations is stressed. In Sec. VIII, we conclude this paper and briefly compare our results with other theoretical surface calculations and with experiment.

II. BULK ELECTRONIC STRUCTURE OF TiO_2

The bulk unit cell of TiO_2 is shown in Fig. 1(a). It contains two Ti cations and four O anions. The Bravais lat-

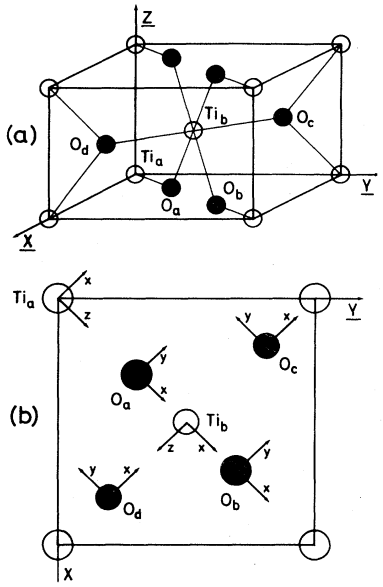

FIG. 1. (a) Bulk unit cell of TiO_2. (b) Local coordinate systems for titanium atoms Ti_a, Ti_b and oxygen atoms O_a, O_b, O_c, O_d.

tice is tetragonal, with parameters $a=4.594$ and $c=2.959$ Å.[19] The cations are located at positions $\vec{r}(\mathrm{Ti}_a)=(0,0,0)$ and $\vec{r}(\mathrm{Ti}_b)=(a/2,a/2,c/2)$, whereas the four anions are located at $\vec{r}(\mathrm{O}_a)=(ua,ua,0)$, $\vec{r}(\mathrm{O}_b)=((1-u)a,(1-u)a,0)$, $\vec{r}(\mathrm{O}_c)=((\frac{1}{2}-u)a,(\frac{1}{2}+u)a,c/2)$, and $\vec{r}(\mathrm{O}_d)=((\frac{1}{2}+u)a,(\frac{1}{2}-u)a,c/2)$, with $u=0.305$.

Each Ti atom has two O neighbors at a distance $d_1=\sqrt{2}ua=1.980$ Å and four O neighbors at a distance $d_2=[2(\frac{1}{2}-u)^2+(c/2a)^2]^{1/2}a=1.948$ Å. So, each cation is surrounded by a nearly regular octahedron of six anions, and each anion is at the center of a nearly equilateral triangle of cations. The octahedral coordination would be perfect for crystal parameters corresponding to $c/a=2-\sqrt{2}$ and $u=(2-\sqrt{2})/2$. The space group of the rutile structure is D_{4h}^{14} ($P4_2/mnm$), whose irreducible representations, as well as those of its little groups, have been given by Dimmock and Wheeler[20] and by Gay *et al.*[21]

For our surface-electronic-structure study, we need a reliable description of the bulk electronic structure. Theoretical calculations have been performed by Vos[22] and Mattheiss.[23] Vos has worked out a tight-binding Hamiltonian with 17 independent parameters which lead to a bulk band structure in good agreement with electroreflectance measurements. Mattheiss started from nonrelativistic augmented-plane-wave calculations at high-symmetry points of the Brillouin zone to set up a tight-binding scheme for the series of rutile-type materials RuO_2, OsO_2, and IrO_2 (Ref. 23) and TiO_2 (Ref. 24). He used 37 independent parameters, including orbital overlap, in his calculations. The electronic structures obtained by both authors present essentially the same characteristics. Owing to its higher Ti-O interaction parameters, Vos obtained a valence-band width of 5.5 eV (instead of 4.34 eV as obtained by Mattheiss) which is somewhat closer to the experimental values generally accepted (5–6 eV).[25] For this reason, and since it is simpler to handle, we have chosen the Hamiltonian of Vos as a basis for our calculations. Unfortunately, no direct experimental measurements of the energy dispersion relations have been performed for TiO_2, as has been done, e.g., for GaAs.[26] Interactions of Ti $3d$, O $2p$, and O $2s$ orbitals are included up to second-nearest neighbors. The O $2s$ bands are explicitly taken into account, although they are only weakly coupled to the other bands, from which they are separated by a 14-eV gap. Since they are not accessible to most surface-sensitive techniques, they will not be displayed in the following.

It is known that an octahedral ligand field causes the five degenerate Ti d states to split into two states of e_g symmetry and three states of t_{2g} symmetry. This effect will be retrieved in the bulk electronic structure, since the octahedral environment is nearly preserved in the crystal. As suggested by Mattheiss,[23] it is useful to adopt the local coordinate system of Fig. 1(b). The z axis which defines the set of Ti d orbitals is directed along the horizontal Ti—O bonds, whereas y indicates the vertical (001) direction. For the O atoms, the coordinates are chosen so that the p_x and p_z orbitals lay inside the O—Ti—O plane, and interact with the Ti d orbitals through $p\,d\sigma$ and $p\,d\pi$ interactions, whereas for the p_y orbitals, only $p\,d\pi$ interactions are nonzero. With that choice of coordinate, the interpretation of the bulk band structure becomes transparent. In Fig. 2, we show the total bulk density of states (DOS), together with the atom- and orbital-resolved DOS.

We display the contributions from the Ti orbitals of t_{2g} symmetry (zy,zx,x^2-y^2) and of e_g symmetry

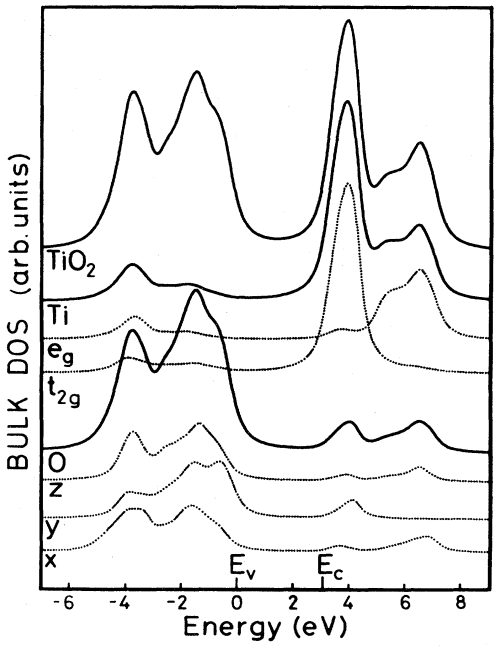

FIG. 2. Bulk density of states of TiO_2, together with partial oxygen (O) and titanium (Ti) densities of states. O DOS's are decomposed into $O_{z,y,x}$ orbital contributions and Ti partial DOS's are decomposed into subbands of $e_g(3z^2-r^2,xy)$ and $t_{2g}(xz,yz,x^2\text{-}y^2)$ symmetry. All DOS's are calculated with a 0.3-eV Lorentzian broadening.

$(xy, 3z^2-r^2)$, and from the O orbitals of x, y, and z symmetry. The energy 0 is taken at the top of the valence band. The titanium and oxygen atomic levels are located at $E_d=2.9$ and $E_p=-1.2$ eV, respectively. As seen on the figure, the Ti states give rise to the two peaks of the conduction band, which are separated by about 3 eV. The higher peak mainly contains contributions of e_g symmetry and is due to the stronger $p\,d\sigma$ interactions between Ti d and O p orbitals. The lower one is dominated by t_{2g} contributions due to the weaker $p\,d\pi$ interactions. The valence band mainly consists of oxygen states, and presents two peaks separated by 2 eV. The lower peak contains only a small O p_y contribution, since it arises from $p\,d\sigma$ interactions, to which p_y orbitals do not contribute. The higher peak mainly arises from $p\,d\pi$ interactions and contains oxygen states of x, y, and z symmetry. The effect of second-nearest-neighbor interactions is to broaden the peaks in the DOS around the atomic levels E_d and E_p. Thus, they play an important role in the study of surface states whose energy is located around the band-gap edges.

It is also worthwhile to note that the Ti partial DOS is non-negligible in the valence-band region, as is the O partial DOS in the conduction-band region. This shows that although it is a polar material, TiO_2 is not completely ionic but has a non-negligible covalent character. Raman spectroscopy[27] and positron annihilation[28] studies lead to an estimate of the ionicity of TiO_2 to 60—70%. As a comparison, the ionicity of GaAs, ZnO, and SnO_2 on the Philips ionicity scale are 0.35, 0.60, and 0.78, respectively.[29]

III. DETERMINATION OF SURFACE ELECTRONIC STRUCTURES

We obtain the surface electronic structure of the various TiO_2 faces by using the scattering theoretical method, whose detailed formal developments can be found in Ref. 16. For unrelaxed surfaces it is sufficient to establish the expression of the bulk Green's function in the layer orbital representation

$$G^b_{l,l'}(\vec{q},E)=\sum_{m,\vec{k}}\frac{\langle l,\vec{q}\,|\,n,\vec{k}\rangle\langle n,\vec{k}\,|\,l'\vec{q}\rangle}{(E+i0+)-E_n(\vec{k})}\ . \tag{1}$$

In this expression, $\vec{q}$ is the two-dimensional Bloch wave vector associated with the surface parallel translational symmetry, $|\,n,\vec{k}\rangle$ and $E_n(\vec{k})$ are, respectively, the eigenvectors and eigenvalues of the bulk Hamiltonian H^b, and $l=(m,\alpha,\mu)$ is a collective index, where m, α, and μ level, respectively, the atomic layer, the atomic orbital, and the atom position in the surface unit cell. The surface is created by removing as many atomic layers as necessary in order to decouple the two remaining half crystals. This is formally achieved by adding to the bulk Hamiltonian a perturbation, whose representation in the layer orbital basis is

$$U_{l,l'}=\begin{cases}\lim\limits_{u\to\infty} u\,\delta_{\alpha,\alpha'}\delta_{\mu,\mu'}\delta_{mm'} & \text{if } m \text{ is a removed layer}\\ 0, \text{ otherwise}\ .\end{cases} \tag{2}$$

The surface states are then obtained by solving the equation

$$D(\vec{q},E)\equiv\det|\,-G^b_{ij}(\vec{q},E)\,|=0\ , \tag{3}$$

where the indices i and j are restricted to the subspaces of removed atoms.

Local densities of states are obtained as partial traces of the surface Green's function $G^s(\vec{q},E)$:

$$N_l(\vec{q},E)=-\frac{1}{\pi}\mathrm{Im}G^s_{ll}(\vec{q},E)\ , \tag{4}$$

where the surface Green's function is obtained by solving Dyson's equation

$$G^s(\vec{q},E)=G^b(\vec{q},E)+G^b(\vec{q},E)UG^s(\vec{q},E)\ . \tag{5}$$

In this paper, we study the (110), (001), and (100) faces of TiO_2. As TiO_2 has the same crystallographic structure as SnO_2, whose surface electronic properties have been determined in Ref. 17, the respective expressions of the bulk Green's function in the different layer orbital representations are those given in this reference. Of course, as eigenvalues and eigenvectors $E_n(\vec{k})$ and $|\,n,\vec{k}\rangle$, we now have to take those corresponding to TiO_2.

IV. THE TiO_2 (110) SURFACE

For the (110) face, we report results for the two models mentioned in the Introduction: the first one terminated by the most compact atomic plane (in the following referred to as model I), and the second one having an additional oxygen layer (referred to as model II). The surface geometry for these two models is represented in Fig. 3.

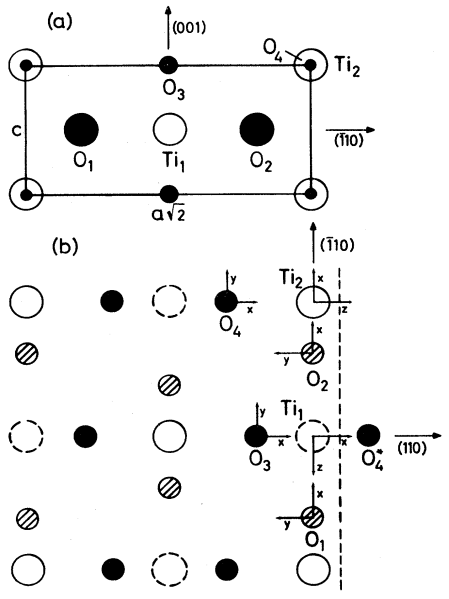

FIG. 3. Surface unit cell of TiO_2(110). (a) Top view ; (b) side view, together with local coordinate systems as defined in Fig. 1. In Model I of TiO_2(110), the surface layer contains the atoms (Ti_1, Ti_2, O_1, O_2). In Model II surface, the top layer contains the atom O_4^*.

The atoms are numbered in a way as to have increasing indices with increasing distance from the surface.

Figure 4 shows the surface band structure for the first model. The shaded areas represent the projection of the bulk band structure on the (110) surface. Solid lines represent true surface states, i.e., states whose energies are inside the gaps or pockets left in the projected bulk band structure. Dashed lines represent surface resonances, which often continue surface states inside the bulk band region. The corresponding surface layer DOS are shown in Fig. 5 for the four high-symmetry points of the surface Brillouin zone (SBZ) Γ, X', M, and X. The solid lines represent the layer-resolved density of states, whereas the dotted lines give the change with respect to the bulk DOS. The upper curve gives the DOS summed over the four atoms of the topmost layer (Ti_1, Ti_2, O_1, O_2), the second curve gives the DOS on the subsurface atom O_3, and the third curve corresponds to the atom O_4 on the next sublayer, where the surface-induced changes of the DOS are already less important. Finally, we display orbital-resolved DOS for Ti_1 and Ti_2 (Fig. 7), and O_1 (equivalent to O_2) and O_3 (Fig. 6). These results allow a detailed discussion of the nature and the localization of the various surface induced features.

The first major conclusion which can be drawn is that no oxygen-derived states are present in the gap, whereas only one titanium-derived state is found approximately 0.15 eV below the conduction-band edge E_c. In the valence-band region, several resonances of dominant O p character appear. None of them extends throughout the Brillouin zone, and their strength, as well as their orbital composition, may vary with surface wave vector $\vec{q}$. In the conduction-band region, a number of surface states

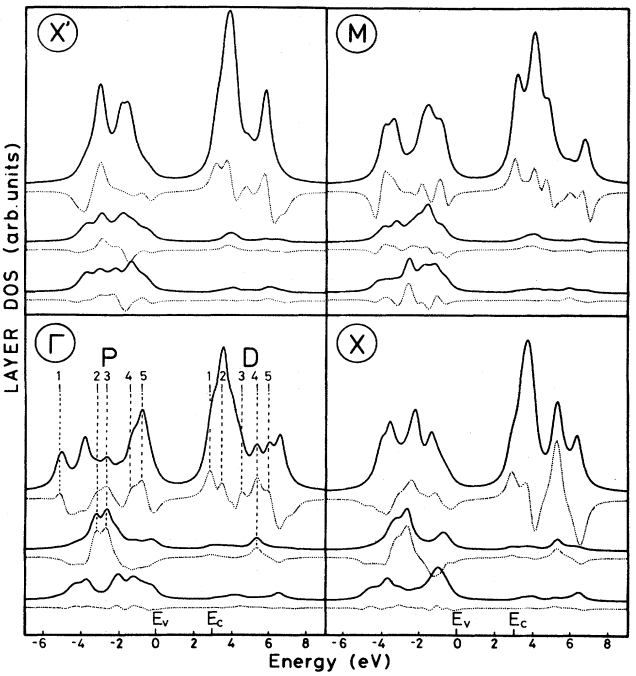

FIG. 5. TiO_2(110)-model I surface. Wave-vector-resolved layer DOS (solid lines) and change with respect to the bulk layer DOS (dotted lines) for the four high-symmetry points Γ, X', M, and X.

and resonances appear, which are of dominant Ti d composition. The orbital composition of these surface features at point Γ can be deduced from Figs. 6 and 7 and is summarized in Table I.

As a consequence of the relatively complex crystallo-

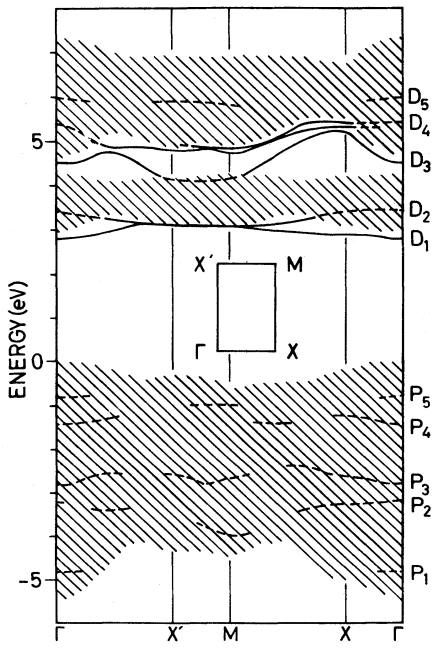

FIG. 4. Projected bulk band structure and surface band structure of TiO_2(110)—Model I surface. Inset: irreducible part of the (110)-surface Brillouin zone.

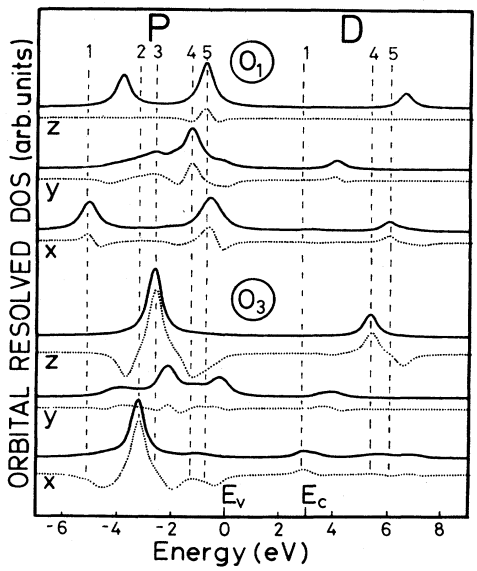

FIG. 6. TiO_2(110)—model I surface. Orbital-resolved atomic DOS's for the surface atom O_1 (O_2) and the subsurface atom O_3, according to the local coordinate system of Fig. 1. Solid lines represent the surface DOS, dotted lines represent the changes with respect to the bulk.

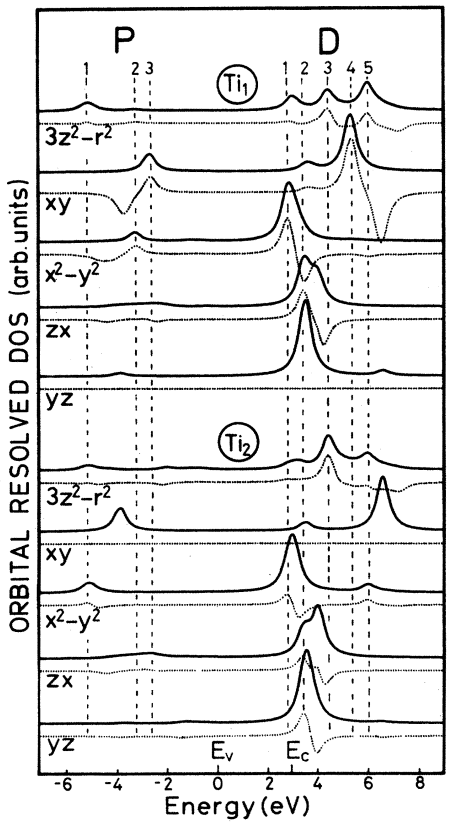

FIG. 7. TiO_2(110)—model I surface. Orbital-resolved atomic DOS's for the surface atoms Ti_1 and Ti_2. The d orbitals are defined in the local coordinate systems of Fig. 1.

graphic structure, the various surface states have their origin in several competing effects: the removal of first-nearest neighbors, which reduces the coordination of the surface atoms and thus causes a shift of bulk states towards the atomic E_d and E_p levels; the suppression of second-nearest-neighbor interactions, which narrows and enhances the peaks near the gap region; and the reduced screening of cation-cation interactions, due to the suppression of surface anions, which causes a repulsion between cation bulk states.

We shall now discuss the surface states at point Γ in some detail. The resonance labeled P_1 is very weak and exists only near point Γ. The two resonances P_2 and P_3 are localized on the subsurface atom O_3 and have, respectively, dominant x and z composition, together with a weak x^2-y^2 and xy admixture from the surface atom Ti_1, which gives them some backbond character. Their origin will be examined below, in connection with the D resonances and surface states. The resonances P_4 and P_5 are localized on the surface atoms O_1 and O_2, and extend only over a small part of the SBZ. As O_1 and O_2 do not lose any nearest neighbors, these resonances are mainly a consequence of the suppression of second-nearest neighbors. Since for the bulk DOS, the second-nearest-neighbor interactions have as a main effect the broadening of the peak around $E_p=-1.2$ eV, the creation of the surface causes resonances to appear, which enhance and narrow this peak.

In the conduction band, five resonances are present at point Γ. The two lowest ones, D_1 and D_2, are of dominant x^2-y^2, xz, and yz character, and the three higher ones, D_3—D_5 have a dominant $3z^2-r^2$ and xy composition. The orbital-resolved changes in the DOS are 0 for yz on Ti_1 and for xy on Ti_2, since these orbitals contribute to bonds which are localized in the surface plane and thus remain unaffected by the creation of the surface.

The two lowest states, D_1 and D_2, are mainly located on Ti_1 and Ti_2, respectively. They result from bulk states which move towards the atomic Ti level at $E_d=2.9$ eV, due to the suppression of anion nearest neighbors. Since Ti_1 is of coordination 4 and Ti_2 of coordination 5, D_1 experiences a larger shift than D_2, and is located at a lower energy. The repulsion between bulk levels caused by Ti-Ti interactions even reinforces this shift, and ultimately pulls down D_1 into the gap. This effect is more important for D_1 than for D_2. Indeed, as can be seen from the orbital character of these surface states, they arise, respectively, from Ti_1-Ti_1 interactions of $d\,d\sigma$ type and Ti_2-Ti_2 interactions of $d\,d\pi$ type along the c axis; Ti_1-Ti_2 interactions, taking place along the diagonal of the surface unit cell, play a minor role, since the atoms involved are separated by a larger distance; furthermore, the Ti_1-Ti_1 interactions are screened only by one intermediate anion (O_3), whereas the Ti_2-Ti_2 interactions are screened by the two surface anions (O_1 and O_3).

The states D_1 and D_2 may be considered as the antibonding states of P_2 and P_3, respectively. P_3 and D_4 are governed by the coupling between the O_3 z and the Ti_1 xy orbitals, which have a relatively large interaction energy (~ 1.4 eV). On the other hand, P_2 and D_1 are governed by the coupling between the x and x^2-y^2 orbitals on the same atoms, which have a weaker interaction energy (~ 0.8 eV). As a consequence, the position of the bulk states from which these surface states originate is further apart from the atomic levels E_p and E_d, and the shift of these bulk states due to the creation of the surface is stronger for P_2 and D_1 than for P_3 and D_4, as seen by examining the position of the corresponding resonances and antiresonances.

On this particular surface, the same calculations have

TABLE I. Orbital and atomic composition of the surface resonances and surface states at point Γ for the compact TiO_2(110) surface (Model I). Orbitals in parentheses are of relatively weak amplitude.

	P_1	P_2	P_3	P_4	P_5	D_1	D_2	D_3	D_4	D_5
Ti_1		(x^2-y^2)	xy			x^2-y^2	xz	$3z^2-r^2$	xy	$3z^2-r^2$
Ti_2	(x^2-y^2)					x^2-y^2	yz,xz	$3z^2-r^2$		(x^2-y^2)
$O_{1,2}$	(x)			y	x,z					(x)
O_3		x	z			(x)			z	

been performed with the tight-binding parameters of Vos replaced by those of Mattheiss. The weaker Ti—O interaction parameters lead, as mentioned above, to a narrowing of the valence band and the conduction band. For the DOS spectra, we obtain the same characteristic features, the position of the resonances and antiresonances being only slightly shifted as compared to the results shown here.

Let us now turn to the discussion of model II, where a layer of oxygen atoms, labeled O_4, is added. As an illustrative example, we show in Fig. 8 the layer DOS at point Γ. By comparison with Fig. 5, it is seen that the adsorption of an additional O atom strongly reduces the amplitudes of the DOS changes on the surface atoms Ti_1, Ti_2, O_1, and O_2, as an effect of bond saturation. The effect is most pronounced for Ti_1, where the coordination is changed from 4 to 6, whereas it is less pronounced for Ti_2 which remains of coordination 5 (see also Fig. 12). The reduced coordination of the O_4 atom (2 instead of 3 in the bulk) has as its only effect the production of a broad resonance level between -2 and -1 eV. No dangling-bond state is created, as in the case of covalent semiconductors (see Ref. 16). On the subsurface atom O_5, the surface resonances P_2 and P_3 present in model I have now disappeared.

The major trends obtained for (110) are also found on the other faces, and the interpretation of the surface DOS curves may be performed along similar lines. We will thus only briefly discuss their properties, insisting on typical features related to the surface atomic structure.

V. THE TiO_2(001) SURFACE

As already mentioned in the Introduction, only one ideal surface model is possible for the (001) face. Each plane contains one Ti and two O atoms per unit cell, and successive layers differ only by a rotation of 90° from one another. As a consequence, the surface unit cell contains one Ti atom, of coordination 4, and two O atoms, of coordination 2. In Fig. 9, we present the wave-vector-resolved surface layer DOS at three different high-symmetry points, Γ, X, and M (which is equivalent to M'), in order to show marked differences which exist between DOS at various $\vec{q}$ values. The wave-vector-integrated surface layer DOS is also displayed.

The major conclusion is again that there are no bound surface states inside the gap. The marked features are O p-derived resonances in the valence-band region and Ti d—derived resonances in the conduction-band region. The creation of the surface has as the main effect the shift of bulk states from the bottom of the valence band and from the top of the conduction band towards, respectively, higher and lower energies (notice the strong antiresonances below -3 eV and above 6 eV). These shifted states reinforce the peaks around the O p level in the valence band and the Ti d level in the conduction band. The $\vec{q}$ integration smooths the DOS curves and reduces the fine structures appearing in $\vec{q}$-resolved spectra.

VI. THE TiO_2(100) SURFACE

Figure 10 shows the geometrical configuration of a TiO_2(100) surface terminated by a cation layer (referred to as model I). Furthermore, we have studied the surfaces obtained by adding one (model II) or two (model III) additional layers of oxygen atoms (labeled O_3^* and O_4^*, respec-

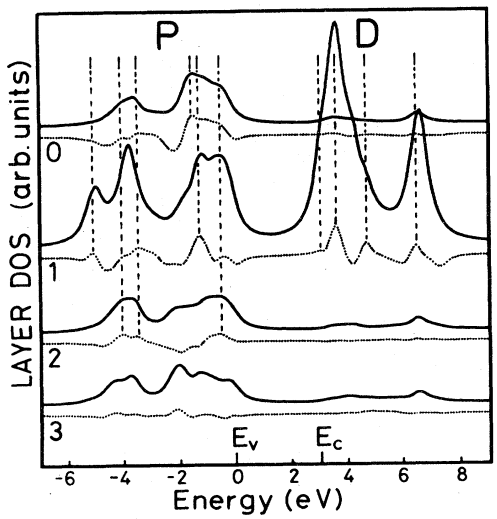

FIG. 8. TiO_2(110), oxygen-terminated surface (model II). Wave-vector-resolved layer DOS (solid lines) and change with respect to the bulk layer DOS (dotted lines) at Γ.

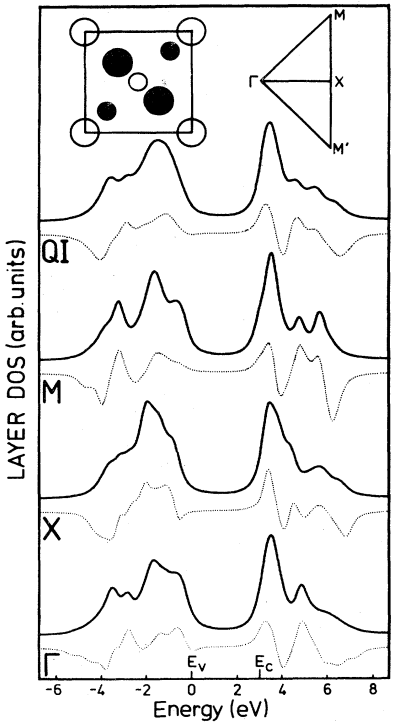

FIG. 9. TiO_2(001). Wave-vector-resolved DOS (full lines) and change with respect to the bulk DOS (dotted lines) at points Γ, X, M, and wave-vector-integrated DOS and change in DOS(QI). Inset: (001)-surface unit cell and irreducible part of (001) SBZ.

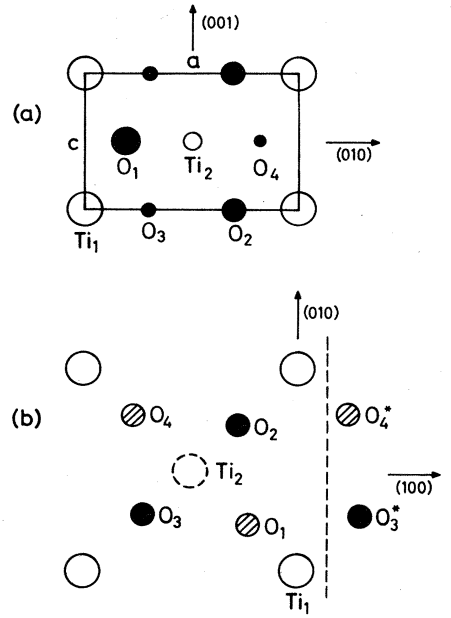

FIG. 10. Surface unit cell of TiO_2(100). (a) Top view of model I surface; (b) side view. In models I, II, and III, the outer surface plane contains, respectively, the atoms Ti_1, O_4^*, and O_3^*.

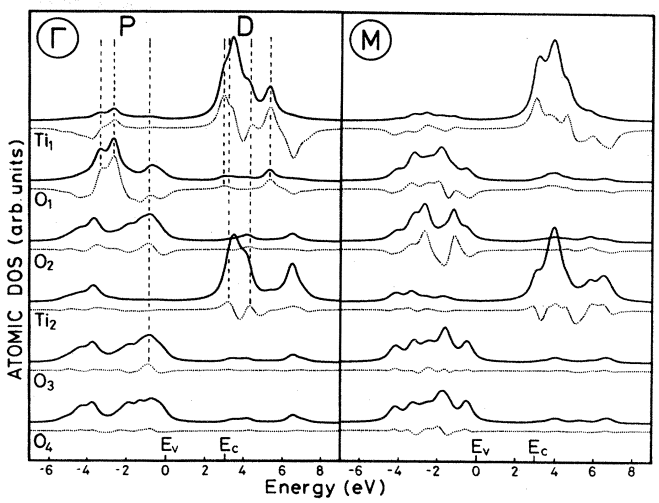

FIG. 11. TiO_2(100)—Ti terminated (model I). Layer DOS (solid lines) and change with respect to bulk DOS (dotted lines) at points Γ and M.

tively). As typical results, we show in Fig. 11 the wave-vector-resolved density of states at Γ and M for the Ti-terminated surface, where the surface cation is now of coordination 3. The DOS is shown on the first six atoms, allowing us to study the DOS changes as one moves towards the crystal. Again, the gap is free of oxygen-derived states. A Ti-derived surface state follows closely the lower border of the projected conduction band, reaching at X a maximum separation of about 0.15 eV below E_c. In the valence-band region, there are again O p resonances located on the subsurface oxygen atom O_1, and the conduction-band region contains Ti d resonances of e_g and t_{2g} symmetry on the surface cation Ti_1. The DOS on O_1 and point Γ resembles closely that of the subsurface atom O_3 on the (110) face; the change in DOS has a double peak at energies −3.20 and −2.55 eV. For the atoms on the next two layers (O_3 and Ti_2) the DOS change is less pronounced, and it has only a weak structure on the atoms of the fifth and sixth layer, as was to be expected.

In Fig. 12, Model I is compared with Models II and III, by displaying the atomic DOS at point Γ for the topmost atoms. Since the atomic configuration of Ti_1, which was 3 in Model I, increases to 5 and 6 for Models II and III, respectively, the DOS changes on this atom are corre-

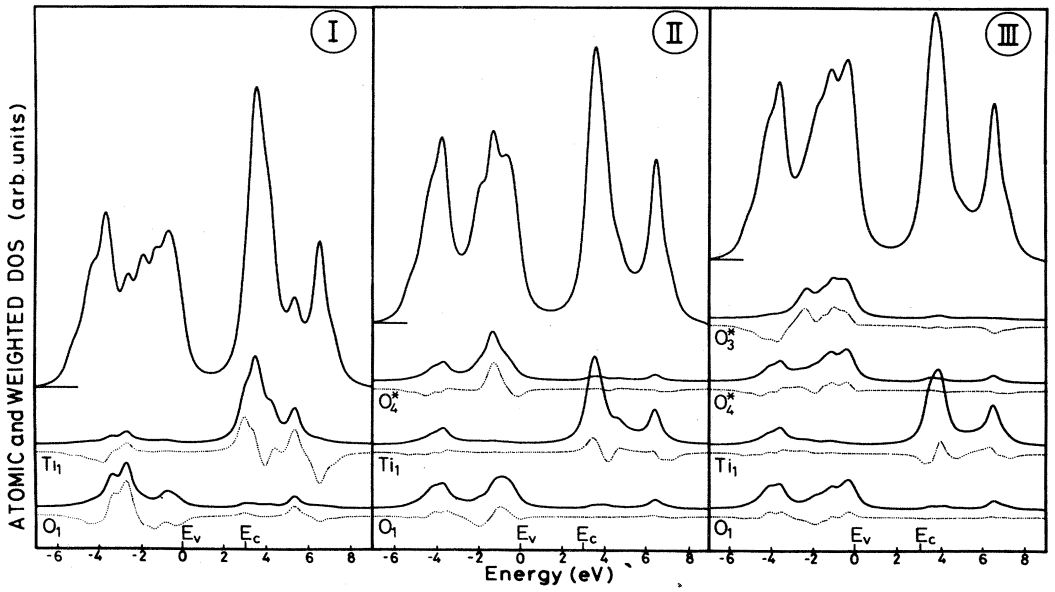

FIG. 12. TiO_2(100). Layer DOS (solid lines) and change with respect to the bulk DOS (dotted lines) at point Γ for the three model surfaces terminated, respectively, by Ti_1, O_4^*, and O_3^*. The upper curve in each panel is the weighted DOS at Γ.

spondingly attenuated. The same is true for O_1, where the strong features at -3.2 and -2.55 eV completely disappear when further oxygen layers are added. In Model II, there is only one strong resonance at -1.5 eV on the surface oxygen atom O_4. This resonance is due to the fact that O_4 has lost one of its three bulk-nearest-neighbor cations. In Model III, the surface oxygen O_3 has lost two of its three neighbor cations, and as a consequence, it carries a resonance at -2.5 eV and a broad peak around -1 eV. However, as for (110) Model II, the surface oxygens may never give rise to gap states, whatever modifications their environment experiences.

On Fig. 12, we also show the weighted DOS's at point Γ, obtained by summing up all layer DOS's multiplied by an exponential decay factor, for which we have taken a decay length of 7 Å. For the valence-band region, this weighted DOS could be compared with an angle-resolved photoemission spectrum for normal emission. The spectra obtained show the same dominant two-peak structure for the three surface models. Addition of surface oxygen causes an enhancement of the higher peak around -1 eV, whereas the lower peak remains nearly unchanged. The fine structures which differentiate the three spectra could be retrieved experimentally only with a very sharp resolution.

VII. COMPARATIVE DISCUSSION OF THE SURFACE ELECTRONIC PROPERTIES

For the various surface orientations and surface models studied, the following common features have been found.

(1) None of the surfaces presented here shows oxygen-derived surface states in the optical gap.

(2) Ti d—derived surface states occur for several surfaces, but those located inside the gap are separated at maximum by 0.2 eV from the conduction-band edge.

(3) By creation of the surface, oxygen p—derived resonances are induced in the valence-band region and Ti d resonances in the conduction-band region. Their localization, composition, and intensity depend on the wave vector $\vec{q}$, the surface atomic composition, and the surface orientation.

(4) By analyzing the energetic position of the resonances and antiresonances, as well as their atomic and orbital composition, it is seen that the O p— and Ti d—derived resonances are primarily due to the cut of nearest-neighbor interactions. Second-nearest-neighbor interactions have a non-negligible effect, either by direct interaction, or by interaction through an intermediate atom (e.g., Ti-mediated O—O interaction). These mediated interactions lead in some cases to a screening of direct second-nearest-neighbor interactions, as does O for the Ti—Ti interactions, and the removal of intermediate anions by creation of the surface strongly enhances the cation-cation interactions. The relative importance of these effects is difficult to determine quantitatively but the main effect of surface creation is to shift bulk states towards the atomic levels E_p and E_d.

Differences from one surface type to another may be explained by the nature of the surface atoms, their relative position, and their coordination. The anion coordination influences the surface resonances located on O. These resonances have, however, a weaker amplitude than those located on Ti atoms. The effect of cation coordination is more pronounced. It is illustrated in Fig. 13, where the atomic DOS's at Γ are displayed for various Ti atoms on different surfaces. The curves are ordered by increasing coordination. It is seen that the lower the coordination, the stronger the amplitude of the DOS changes: only moderate for coordination 6 and 5, it becomes important for coordination 4 and 3, as intuitively expected. In the two latter cases, two strong antiresonances reveal the bulk states from which they originate, clearly indicating that they are due to the suppression of $p\,d\sigma$ and $p\,d\pi$ nearest-neighbor bonds. If one examines the energetic position of the lowest Ti state on various faces, one sees that this state is located at 2.84 eV for Ti_1 on (110) model I, at 2.94 eV on (100) model I and at 3.17 eV on (001). This variation over a range of 0.33 eV can be explained by the repulsion between Ti states which is more or less pronounced depending on the reduced screening of the cation-cation interactions due to the removal of anion nearest neighbors. Indeed, on the (110) and (100) surfaces, the nearest-neighbor distance between two Ti atoms in the surface layer is $c=2.96$ Å, whereas it is $a=4.59$ Å on the (001) surface.

The general trends summarized above are correlated with the relatively ionic character of TiO_2. No occupied O p gap states have been obtained for SnO_2 (Ref. 17) and ZnO (Ref. 15), materials of comparable ionicity. For covalent materials such as Si, Ge, or even GaAs, the surface creation requires bond charges to be cut, which causes the bulk states to shift towards the hybrid sp^3 level in the midgap, giving rise to dangling-bond states in the band gap. For ionic materials, on the contrary, the creation of

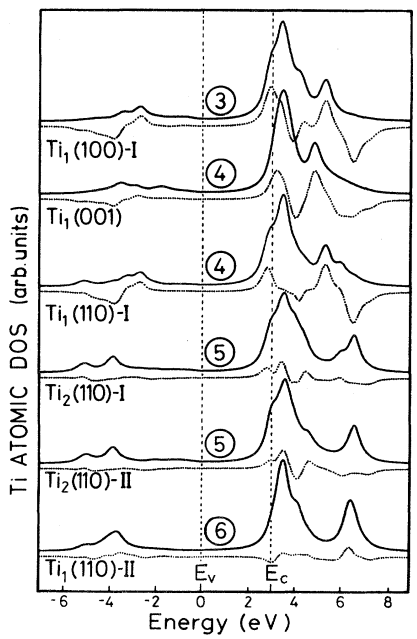

FIG. 13. Atomic-resolved DOS (solid lines) and change with respect to the corresponding bulk DOS (dotted lines) at point Γ for surface Ti atoms on various TiO_2 surfaces. Coordination of surface cations is indicated by numbers in circles.

the surface consists mainly in the separation of atoms which carry an important ionic charge and henceforth are not expected to yield such dangling-bond states in the gap.

VIII. CONCLUSION

We have studied the surface electronic structure of ideal, defect-free TiO_2(110), (001), and (100) surfaces using the scattering theoretical method. For each surface orientation, different surface compositions were considered, depending on the atomic plane which terminates the crystal. The models chosen are the most probable to occur in various experimental conditions. The main result of our theory is that the gap is nearly free of surface states. Only a Ti *d* state, very close to the conduction-band edge, appears for some surfaces; O *p* states are always absent. Inside the valence and conduction bands, respectively, O *p* and Ti *d* resonances occur.

These results are in accordance with the experimental EELS and UPS data discussed in the Introduction,[6,10] which indicate no presence of gap states for clean, defect-free TiO_2 surfaces. Only surface defects were able to produce states at energies below 3 eV. This seems to be confirmed by some preliminary calculations. By removing all O_1 atoms from the (110) face (see Fig. 3) we obtain a gap state at 2.75 eV, and removing in addition all O_2 atoms yields a state at 2 eV. However, such surfaces with regular arrays of defects are unlikely to be stable, and in order to consider more realistic systems, we are currently performing investigations on isolated surface defects. Our results disagree with former theoretical calculations,[30] which concluded on the existence of O *p*—derived gap states, probably related to the use of finite slabs or clusters in the surface-electronic-structure calculations.

The effects of surface relaxation could be taken into account within the framework of the STM,[18] but knowledge of the exact atomic positions is needed from experiment, which is currently unavailable. However, for ionic materials, no drastic changes are to be expected from relaxation, as it results from studies on ZnO $(10\bar{1}0)$.[15]

ACKNOWLEDGMENTS

We are indebted to Dr. L. F. Mattheiss for sending us results of unpublished bulk band structures on TiO_2. One of us (S.M.) would like to thank the Belgian Fonds National de la Recherche Scientifique for financial support.

[1]A. J. Bard, J. Photochem. 10, 59 (1979); Science 207, 139 (1980).
[2]G. N. Schrauzer and T. D. Guth, J. Am. Chem. Soc. 99, 7189 (1977); I. Izumi, F. R. F. Fen, and A. J. Bard, J. Phys. Chem. 85, 218 (1981).
[3]W. Göpel, G. Rocker, and R. Feierabend, Phys. Rev. B 28, 3427 (1983).
[4]E. A. Grant, Rev. Mod. Phys. 31, 646 (1959).
[5]V. E. Henrich, Prog. Surf. Sci. 9, 143 (1979); in *Proceedings of the IXX-IVC/V-ICSS,* edited by J. L. de Segovia (A.S.E.V.A., Madrid, 1983), p. 100; Prog. Surf. Sci. 14, 175 (1983).
[6]R. H. Tait and R. V. Kasowski, Phys. Rev. B 20, 5178 (1979).
[7]Y. W. Chung, W. J. Lo, and G. A. Somorjaj, Surf. Sci. 64, 588 (1977); W. J. Lo, Y. W. Chung, and G. A. Somorjaj, Surf. Sci. 71, 199 (1978).
[8]G. Van Steertegem, J. Vandermolen, H. Van Hove, and A. Neyens (private communication).
[9]V. E. Henrich, G. Dresselhaus, and H. J. Zeiger, Phys. Rev. Lett. 36, 1335 (1976).
[10]V. E. Heinrich and R. L. Kurtz, Phys. Rev. B 23, 6280 (1981).
[11]L. E. Firment, Surf. Sci. 116, 205 (1982).
[12]S. Munnix and M. Schmeits, Surf. Sci. 126, 20 (1983); Phys. Rev. B 28, 7342 (1983).
[13]E. de Frésart, J. Darville, and J. M. Gilles, Solid State Commun. 37, 13 (1980); Surf. Sci. 126, 518 (1983).
[14]See, for example, R. J. Meyer, C. B. Duke, A. Paton, A. Kahn, E. So, J. L. Yeh, and P. Mark, Phys. Rev. B 19, 5194 (1979).
[15]I. Ivanov and J. Pollmann, Phys. Rev. B 24, 7275 (1981); D. H. Lee and J. D. Joannopoulos, *ibid.* 24, 6899 (1981).
[16]J. Pollmann and S. T. Pantelides, Phys. Rev. B 18, 5524 (1978).
[17]S. Munnix and M. Schmeits, Phys. Rev. B 27, 7624 (1983).
[18]M. Schmeits, A. Mazur, and J. Pollmann, Phys. Rev. B 27, 5012 (1983).
[19]S. C. Abrahams and J. L. Bernstein, J. Chem. Phys. 55, 3206 (1971).
[20]J. O. Dimmock and R. G. Wheeler, Phys. Rev. 127, 391 (1962).
[21]J. G. Gay, W. A. Albers, and F. J. Arlinghaus, J. Phys. Chem. Solids 29, 1449 (1968).
[22]K. Vos, J. Phys. C 10, 3917 (1977).
[23]L. F. Mattheiss, Phys. Rev. B13, 2433 (1976).
[24]L. F. Mattheiss (private communication).
[25]S. P. Kowalczyk, F. R. McFeely, L. Ley, V. T. Gritsyna, and D. A. Shirley, Solid State Commun. 23, 161 (1977).
[26]T. C. Chang, Y. A. Knapp, M. Aono, and D. E. Eastmann, Phys. Rev. B 21, 3513 (1980).
[27]G. A. Samara and P. S. Peercy, Phys. Rev. B 27, 1131 (1973).
[28]D. Tsur, M. Blau, and M. Wegner, J. Phys. C 7, 1257 (1974).
[29]B. F. Levine, J. Chem. Phys. 59, 1463 (1973).
[30]R. V. Kasowski and R. H. Tait, Phys. Rev. B 20, 5168 (1979); M. Tsukuda, C. Satoko, and H. Adachi, J. Phys. Soc. Jpn. 47, 1610 (1979).